

See discussions, stats, and author profiles for this publication at: <https://www.researchgate.net/publication/51068020>

# Synergistic Effects of Mixed Aromatic Counterions on Nanostructures and Drag Reducing Effectiveness of Aqueous Cationic Surfactant Solutions

ARTICLE *in* THE JOURNAL OF PHYSICAL CHEMISTRY B · MAY 2011

Impact Factor: 3.3 · DOI: 10.1021/jp201386v · Source: PubMed

---

CITATIONS

9

READS

39

## 5 AUTHORS, INCLUDING:



[Wu Ge](#)

The Ohio State University

10 PUBLICATIONS 129 CITATIONS

[SEE PROFILE](#)



[Haifeng Shi](#)

The Ohio State University

8 PUBLICATIONS 83 CITATIONS

[SEE PROFILE](#)



[Jacques L Zakin](#)

The Ohio State University

117 PUBLICATIONS 2,064 CITATIONS

[SEE PROFILE](#)

# Synergistic Effects of Mixed Aromatic Counterions on Nanostructures and Drag Reducing Effectiveness of Aqueous Cationic Surfactant Solutions

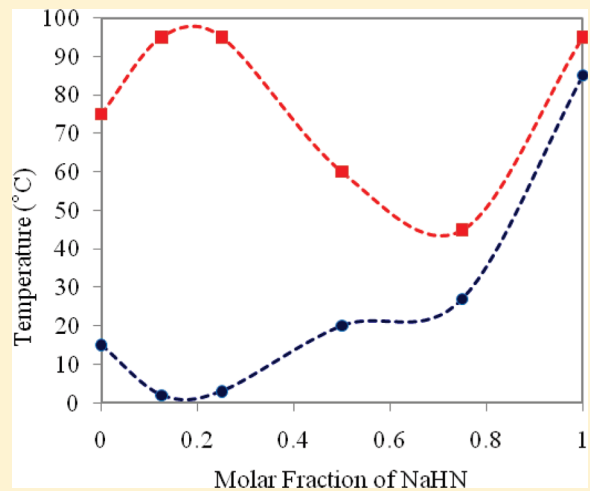
Wu Ge,<sup>†</sup> Haifeng Shi,<sup>†</sup> Yeshayahu Talmon,<sup>‡</sup> David J. Hart,<sup>§</sup> and Jacques L. Zakin<sup>\*†</sup>

<sup>†</sup>Department of Chemical and Biomolecular Engineering, The Ohio State University, Columbus, Ohio 43210, United States

<sup>‡</sup>Department of Chemical Engineering, Technion-Israel Institute of Technology, Haifa, 32000, Israel

<sup>§</sup>Department of Chemistry, The Ohio State University, Columbus, Ohio 43210, United States

**ABSTRACT:** Drag reduction effectiveness of two dilute quaternary ammonium surfactant aqueous solutions with different pairs of mixed aromatic counterions was investigated along with their micellar nanostructures revealed by cryo-TEM imaging, zeta potential, particle size, and <sup>1</sup>H NMR measurements. Certain combinations of aromatic counterion mixtures showed significant synergistic effects. They dramatically improved drag reduction effectiveness relative to either single aromatic counterion. Using mixed aromatic counterions with different sizes and binding abilities, the effective drag reducing temperature range can be significantly expanded and higher shear stress stability can be achieved. The synergistic effects are believed to be induced by increased degree of branching in the surfactant micellar networks as shown by cryo-TEM images.



## INTRODUCTION

Thread-like micelles (TLMs) and their networks are generally believed to be responsible for many of surfactant solutions' interesting flow phenomena, such as turbulent drag reduction, viscoelasticity, shear thickening, and flow birefringence.<sup>1</sup> With soaring energy costs, surfactant drag reduction, which is suitable for energy efficient district cooling/heating systems, has attracted more and more research effort. Due to their excellent drag reducing ability, broad availability, low concentration requirements, and general insensitivity to ionic metal impurities in water, cationic surfactants have received the most attention in drag reduction studies during the past two decades.<sup>2,3</sup> Organic counterions added to dilute cationic surfactant aqueous solutions are effective in inducing and stabilizing TLM formation at relatively low counterion to surfactant molar ratios, thereby promoting their drag reducing effectiveness. The interactions of the cationic surfactant and organic counterion can be enhanced by tuning either or both of them, structurally and/or by concentration and molar ratio, to tailor-make highly efficient drag reducing systems suitable for different applications. The focus of past research on cationic surfactant drag reducing systems has been on the effects of cationic surfactant structure such as the length,<sup>4–6</sup> the odd or even number of carbons,<sup>6,7</sup> the saturation/unsaturation of C–H bonds<sup>5</sup> and the cis/trans configurations<sup>8</sup> of their hydrophobic alkyl chains, and the effects of

hydrophilicity and geometric size of their headgroups,<sup>9</sup> as well as the effects of counterion structure and concentrations of cations and counterions.<sup>10,11</sup>

A surfactant solution is considered drag reducing *significant* or *effective*, if the percentage drag reduction (eq 1) in turbulent flow is 50% or more. Mixed surfactant systems such as cationic surfactants with different chain lengths,<sup>6</sup> cationic/anionic systems,<sup>12,13</sup> and zwitterionic/anionic systems<sup>14</sup> have been shown to enhance drag reduction effectiveness, especially to expand the effective drag reducing temperature range (EDRTR), which is enveloped by the two critical temperature curves shown on an EDRTR graph (see Figures 1 and 2, for example). This figure shows the upper critical temperature ( $T_{UC}$ ), above which the TLMs are too short to induce significant drag reduction, and the lower critical temperature ( $T_{LC}$ ), below which the solution loses its significant drag reducing ability, due to phase separation caused by poor surfactant solubility. For mixed cationic surfactants with different chain lengths (C22 and C12), it was found that the addition of C12 to C22 lowered the  $T_{LC}$  greatly, while the  $T_{UC}$  was only slightly reduced.<sup>6</sup>

**Received:** February 11, 2011

**Revised:** March 28, 2011

**Published:** April 21, 2011

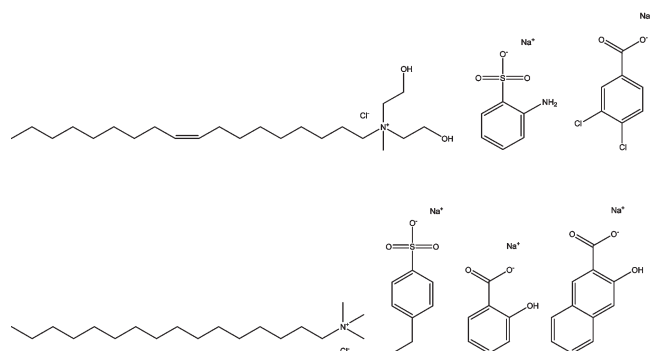


**Figure 1.** Materials studied, first row from left to right: EO 12 (only the main component, Oleylbis(hydroxyethyl)methylammonium chloride is shown), sodium aniline-2-sulfonate (NaA2S) and sodium 3,4-dichlorobenzoate (Na34ClB), second row from left to right: cetyltrimethylammonium chloride (CTAC), sodium 4-ethylbenzenesulfonate (NaEBS), sodium salicylate (NaSal), and sodium 3-hydroxy-2-naphthoate (NaHN).

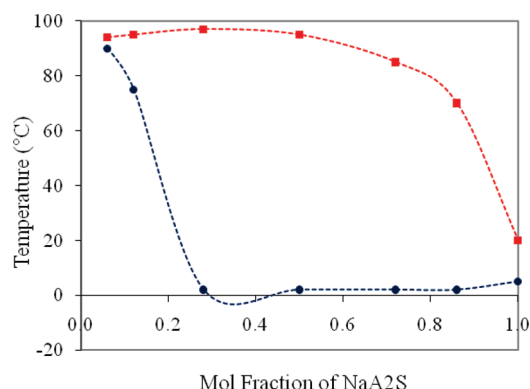


**Figure 2.** Effective drag reducing temperature range (EDRTR) for 5 mM EO12 with 12.5 mM NaA2S and Na34ClB. ■:  $T_{UC}$ , ●:  $T_{LC}$ . EDRTR is the height between the dotted lines. (5 mM EO12 with 12.5 mM Na34ClB was tested to be not drag reducing effective and cannot be presented in the figure).

Small inorganic counterions such as  $\text{Cl}^-$  or  $\text{Br}^-$  bind to the cationic micelles only at the interfacial level (Stern layer), and mildly mitigate the headgroup repulsions, while aromatic counterions such as salicylate or tosylate can intercalate deeply into the micelle core as revealed in NMR studies,<sup>11,15–17</sup> leaving part of their delocalized  $\pi$ -electron aromatic ring and the negatively charged sulfonate, or carboxylate group, in close proximity to the positively charged headgroups and effectively hydrated by water molecules near the micelle surface, thus greatly stabilizing and promoting the TLMs.<sup>18,19</sup> Certain aromatic counterions that can form strong intramolecular hydrogen bonds, such as salicylates,<sup>20</sup> have been found to be very effective in inducing drag reduction.<sup>4</sup> In mixed counterion systems where inorganic counterions compete with organic counterions for binding sites at the micellar surface, the penetrating organic counterions dominate in the competition according to a *two site* model,<sup>11</sup> which states that penetrating organic counterions also bind in the Stern layer, and can replace the absorbed small inorganic counterions.<sup>18,21</sup> The binding selectivity of aromatic counterions was reported to be at least 1 order of magnitude larger than that of  $\text{Br}^-$  which is a strong binding inorganic counterion.<sup>22</sup> It was pointed out that for cationic surfactant solutions containing penetrating aromatic

counterion(s), inorganic counterions do not have a significant effect on drag reduction, unless they are present at high concentrations (more than 10 to 1 molar ratio over the surfactant concentration), where they may moderately improve drag reduction.<sup>4</sup> In this research, the negligible effects of the small inorganic anions that come with the cationic surfactants (1 to 1 ratio) are therefore ignored.<sup>11</sup>

Since aromatic counterions play an important role in the dynamics of the formation of cationic surfactant TLMs and their networks, we postulated that certain mixed aromatic counterion systems might be more effective as TLM promoters than single counterions. To our knowledge, there have been no previous reported investigations of the effect of mixed organic counterions on drag reduction effectiveness. In this work, we report the synergistic effects of mixtures of selected aromatic counterions with different sizes and binding abilities on the drag reducing effectiveness of two quaternary ammonium surfactant solutions (cetyltrimethylammonium chloride or CTAC, and Ethoquad O12 or EO12, a mixture of alkyl bis(hydroxyethyl) methyl ammonium chloride). Various combinations of aromatic counterion pairs were studied; sodium salicylate, (NaSal), sodium 3,4-dichlorobenzoate (Na34ClB), sodium aniline-2-sulfonate (NaA2S), sodium 4-ethylbenzenesulfonate (NaEBS), and sodium 3-hydroxy-2-naphthoate (NaHN) for drag reduction and rheological behavior, as well as for their micellar nanostructures as revealed by cryo-TEM imaging, zeta-potential, particle size,<sup>1</sup>H NMR and rheo-optic measurements.

## EXPERIMENTAL SECTION

**Materials.** EO12 was donated by Azko Nobel, Inc. It came as 75 wt % active component dissolved in propylene glycol. The EO12 alkyl group has about 75% of unsaturated *cis*-C18, 14% of saturated C18 and about 10% of unsaturated and saturated C16. See Figure 1 for structure of its main component. CTAC was purchased from Nanjing Robiot Co., Ltd., with a label purity of 99%.

3,4-Dichlorobenzoic acid (99%), aniline-2-sulfonic acid (95%), 4-ethylbenzenesulfonic acid (95%), and 3-hydroxy-2-naphthoic acid (98%) were purchased from Sigma-Aldrich. NaOH (purchased from Mallinckrodt Chemicals, AR grade) was used to neutralize each acid through titration (pH value of each sample was monitored and controlled to be between 6 and 8). NaSal was purchased from Sigma-Aldrich with a label purity of 99%.

All chemicals were used as received. Except for drag reduction measurements, all tests were performed at room temperature (25 °C). The molar ratio between total concentration of each pair of aromatic counterions and surfactant was fixed at 2.5 except for <sup>1</sup>H NMR. Distilled water was used as solvent except for NMR tests, where D<sub>2</sub>O was used. Samples for drag reduction tests (5 mM cationic surfactant concentration and 12.5 mM total concentration) were stirred continuously for 8 h followed by 24 h of rest before measurement, to ensure that they reached equilibrium. Drag reduction samples for cryo-TEM measurements had longer rest times of about 1 to 2 weeks, because of the time needed for international delivery to the test facility in Israel.

**Drag Reduction.** Drag reduction percentage was obtained by comparing the friction factor of test solutions,  $f$ , measured with a closed flow loop, with the friction factor of the solvent (water),  $f_s$ , calculated from von Karman equation at the same solvent

Reynolds number.

$$\%DR = \frac{f_s - f}{f_s} \times 100 \quad (1)$$

Details on the drag reduction flow loop and the calculation procedures can be found in previous publications.<sup>11,23,24</sup>

**<sup>1</sup>H NMR.** <sup>1</sup>H NMR experiments for the CTAC systems in D<sub>2</sub>O were performed with a Bruker DRX-600 MHz (14.14 T) NMR spectrometer at the Campus Chemical Instrument Center of The Ohio State University. First, <sup>1</sup>H NMR spectra of each aromatic counterion alone in D<sub>2</sub>O as well as <sup>1</sup>H NMR spectrum of a 5 mM CTAC D<sub>2</sub>O solution were obtained. Then, a series of aromatic counterion mixtures was added to the CTAC solution. Overall counterion-to-surfactant ratio was selected as 0.3 to avoid significant line broadening. All NMR samples were prepared following the same titration, stirring and resting procedures described in the Materials section, and were run in standard NMR tubes at 25 °C.

**ζ Potential and Particle Size.** The ζ potential and particle size measurements were performed with a Zetasizer Nano particle analyzer, Nano ZS90, from Malvern Instruments, Inc. Nano ZS90 performs size measurements using dynamic light scattering (DLS), which measures Brownian motion and relates that to the size of the particles, by illuminating the particles with a laser beam and analyzing the intensity fluctuations in the scattered light. It calculates the ζ potential by determining the electrophoretic mobility and then applying the Henry equation. The electrophoretic mobility is obtained by performing an electrophoresis experiment on the sample, and measuring the velocity of the particles using laser Doppler velocimetry (LDV). The Nano ZS90 measures particle size from 1 nm to 3 μm, and ζ potentials for particles in the size range of 5 nm to 10 μm.

**Cryo-TEM.** Cryo-TEM images of the CTAC systems at 25 °C were taken at Technion-Israel Institute of Technology. Sample preparation was previously described.<sup>11</sup> Details of the cryo-TEM imaging technique can be found elsewhere.<sup>25,26</sup>

## RESULTS AND DISCUSSION

**Drag Reduction.** The 5-mM EO12 aqueous solutions with 12.5 mM mixtures of NaA2S and Na34ClB were tested for drag reduction. Figure 2 shows the EDRTR for this system. When used in a longer chain (C22) unsaturated cationic surfactant solution, NaA2S is a very effective counterion and gives an EDRTR of 30 to 80 °C,<sup>4</sup> while with EO12, it is only effective from 5 to 20 °C as shown on the right-hand side of Figure 2, where the molar fraction of NaA2S equals 1. When used in a shorter chain (C16) saturated surfactant solution, similar to CTAC, Na34ClB is an effective counterion and gives an EDRTR of 20 to 80 °C,<sup>10</sup> while with EO12, it is not effective as the EDRTR is zero as seen on the left-hand side of Figure 2 when molar fraction of NaA2S is 0. However, mixtures of NaA2S and Na34ClB with EO12 exhibit a significant synergistic effect. The EDRTR is much expanded as shown in Figure 2. At low molar ratios of NaA2S the *T*<sub>LC</sub> curve becomes closer and closer to the *T*<sub>UC</sub> curve, and they converge at 100% Na34ClB, where the drag reduction is not significant.

It should be pointed out that the real EDRTR in Figure 2 may actually be broader at some mixture ratios, as our drag reduction test facility is not pressurized, and can only operate at temperatures below 98 °C to avoid water boiling in the positive displacement pump, and above 2 °C to avoid water freezing.

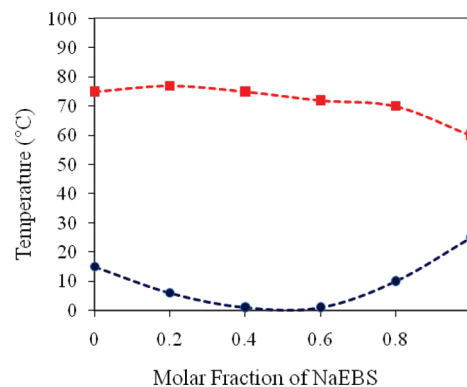


**Figure 3.** Effective drag reducing temperature range (EDRTR) for 5 mM CTAC aqueous solution with 12.5 mM NaSal and NaEBS. ■: *T*<sub>UC</sub>, ●: *T*<sub>LC</sub>. EDRTR is the height between the dotted lines.

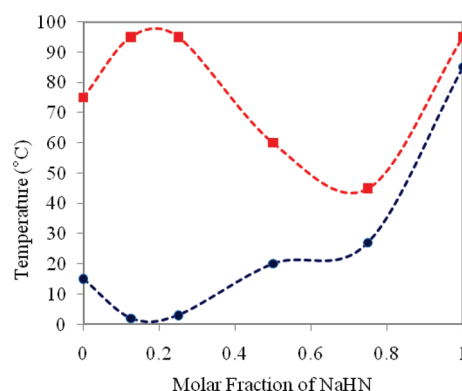


**Figure 4.** Effective drag reducing temperature range (EDRTR) for 5 mM CTAC aqueous solution with 12.5 mM NaSal and NaHN. ■: *T*<sub>UC</sub>, ●: *T*<sub>LC</sub>. EDRTR is the area between the dotted lines.

The 5-mM CTAC aqueous solutions with two pairs of aromatic counterions, NaSal and NaEBS and NaSal and NaHN, both at 12.5 mM total concentration, were also tested for drag reduction. Figures 3 and 4 show expanded EDRTR, demonstrating the synergistic effect of mixing aromatic counterions for both pairs.

Figure 3 shows that the EDRTR expansion of the NaSal and NaEBS mixture is moderate, and is mostly due to the downward expansion of the EDRTR, while there is little increase in the *T*<sub>UC</sub> values. The *T*<sub>LC</sub> curve is symmetric; it has a minimum around the 50–50 ratio, which is also the point where the EDRTR is the broadest for this system.

EDRTR expansion of NaSal and NaHN mixtures is more pronounced, especially around the 20% NaHN point (Figure 4). NaHN, when used as the lone aromatic counterion, is only effective over a narrow temperature range near 90 °C. The gradual addition of NaSal to NaHN lowers the effective range, until about 75% NaHN. At a molar fraction of 20% NaSal, the EDRTR is greatly enlarged. Again, experimental facility limitations did not allow us to find the maximum EDRTR in that region.

Maximum %DR and *τ*<sub>wc</sub>, the critical wall shear stress at which drag reduction reaches a maximum and starts to decrease, are two other important measures of drag reduction effectiveness. Tables 1 and 2 list them at 25 °C for the CTAC systems. From Table 1, we see that the maximum %DR and maximum *τ*<sub>wc</sub> increase for the mixed aromatic counterions of NaSal and NaEBS at all compositions tested. From Table 2 we see the synergistic effect appears to be largest at

**Table 1.** Drag Reducing Effectiveness for 5 mM CTAC Solutions with 12.5 mM of Mixed Aromatic Counterions<sup>a</sup>

counterion ratio [NaSal]: [NaEBS]	maximum %DR	maximum $\tau_{wc}$
	(25 °C)	(25 °C, Pa)
100:0	76	25
80:20	>80	>30
60:40	>80	>30
40:60	>80	>30
20:80	>80	>30
0:100	60	15

<sup>a</sup>The symbol “>” means either the flow rate or the pressure drop is beyond the drag reduction test facility’s measuring range.

**Table 2.** Drag Reducing Effectiveness for 5 mM CTAC Solutions with 12.5 mM of Mixed Aromatic Counterions<sup>a</sup>

counterion ratio [NaSal]: [NaHN]	maximum %DR	maximum $\tau_{wc}$
	(25 °C)	(25 °C, Pa)
100:0	76	25
75:25	>80	>35
50:50	50	28
25:75	68	50
0:100	not drag reducing	not drag reducing

<sup>a</sup>The symbol “>” means either the flow rate or the pressure drop is beyond the drag reduction test facility’s measuring range.

about 25% NaHN composition, where the EDRTR is greatly expanded, maximum %DR is increased, and maximum  $\tau_{wc}$  is projected to be enhanced. However, the values could not be determined due to pumping flow rate limitation. At 50–50 NaSal and NaHN, where a synergistic effect is anticipated, the drag reduction effectiveness is lower than expected, as shown by the relatively low values of maximum %DR and maximum  $\tau_{wc}$ . This result is anomalous. It is possible that this 50–50 counterion mixture has high micellar network density, and is near its saturation point, leading to shear induced phase separation at relatively low shear stress levels in the test facility, causing the solution to lose its drag reducing ability.

**$^1\text{H}$  NMR.** To probe the interactions between the mixed aromatic counterions and surfactant micelles,  $^1\text{H}$  NMR measurements were performed on the two CTAC systems; the results are shown in Figures 5–8. In these figures, CTAC concentration was fixed at 5 mM. To avoid line broadening caused by elongated, bulky and therefore slow moving micellar structures,<sup>16</sup> the total concentration of the aromatic counterion pairs was reduced to 1.5 mM giving a ratio of counterion to surfactant of 0.3, which is relatively low. It is assumed, based on the *two site* model,<sup>11</sup> that at this molar ratio most of the aromatic counterions are bound on the micelles with few left in the bulk solution so free counterions do not affect the locations of the aromatic counterion proton chemical shifts.<sup>16</sup>

Figure 5 shows the ring proton chemical shifts for the aromatic counterions of the CTAC with NaSal and NaEBS system. The spectra on the very top and bottom are for pure NaSal and NaEBS in  $\text{D}_2\text{O}$  without surfactant, respectively. The spectra in between are for the 5 mM CTAC with these two aromatic counterions at different ratios. Upon adding the aromatic counterions to the CTAC solution, all ring protons of both aromatic

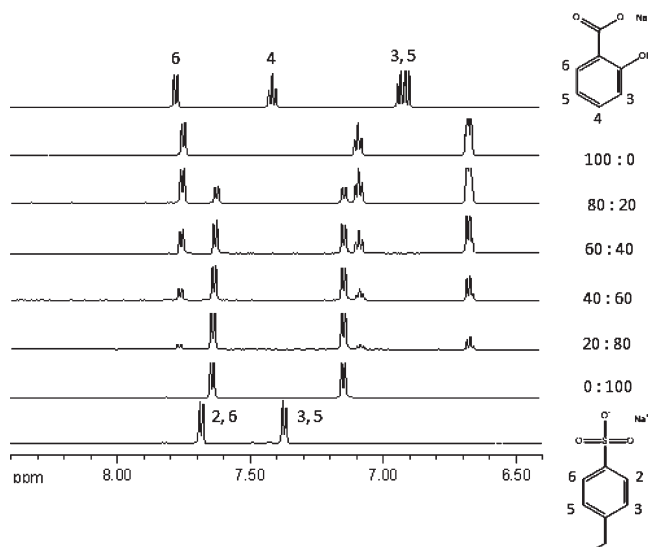


**Figure 5.** Ring proton NMR spectra for 5 mM CTAC with 1.5 mM mixtures of NaSal and NaEBS at 25 °C.

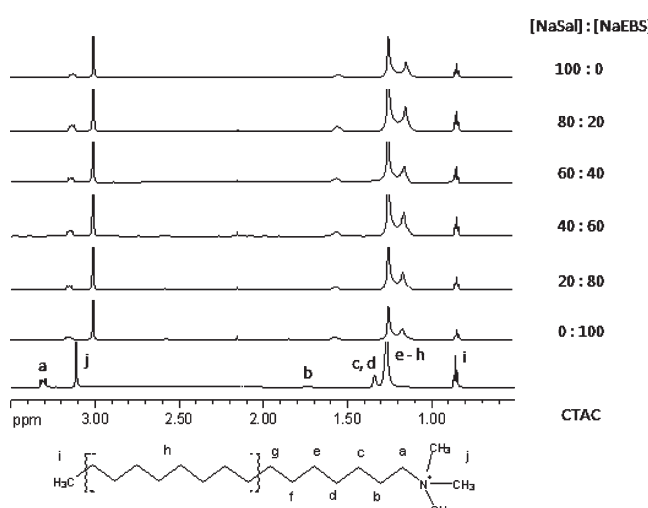


**Figure 6.** Alkyl chain proton NMR spectra for 5 mM CTAC with 1.5 mM mixtures of NaSal and NaEBS at 25 °C.

counterions are shifted upfield. This phenomenon has been observed many times previously<sup>9,11,15,16,27</sup> and is evidence of aromatic counterions’ insertion binding ability. That is, the environmental electron cloud density for the ring protons on the aromatic counterions decreases when the aromatic counterions are transferred from the bulk  $\text{D}_2\text{O}$  phase to the micellar interface with the hydrophobic phenyl ring (NaSal) and p-ethyl-phenyl ring (NaEBS) inserted into the less polar micellar core and the hydrophilic carboxyl group (NaSal) and sulfonate group (NaEBS) in contact with water and/or the cationic headgroup. The orientation of both aromatic counterions follows a “ring first” insertion pattern with the hydrophilic group (carboxyl or sulphonyl) pointing out normal to the micelle-water interface. The distance of a ring proton’s upfield shift is related to where the proton sits, that is, the farther away it is located from the hydrophilic substitution group, the more it shifts upfield. For NaSal, 4H shifts the most, then 3H and 5H. 6H shifts only

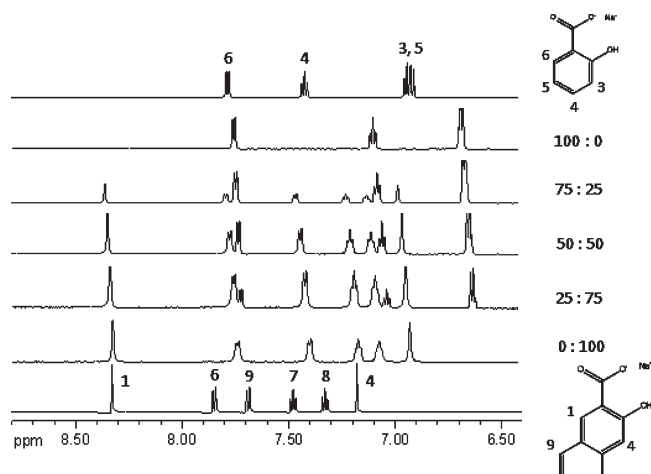


**Figure 7.** Ring proton NMR spectra for 5 mM CTAC with 1.5 mM mixtures of NaSal and NaHN at 25 °C.

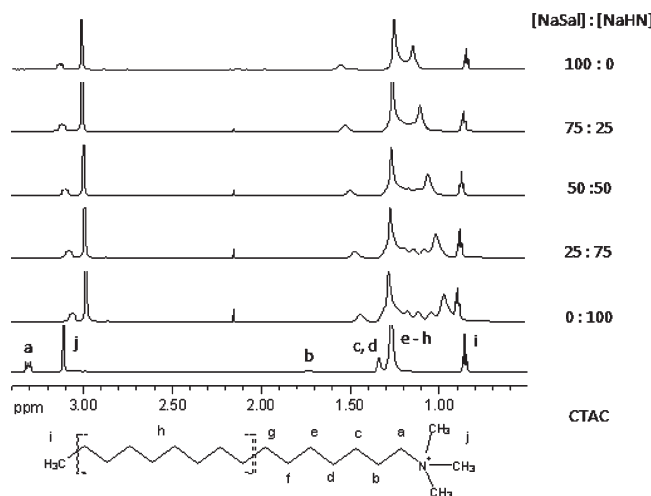


**Figure 8.** Alkyl chain proton NMR spectra for 5 mM CTAC with 1.5 mM mixtures of NaSal and NaHN at 25 °C.

slightly. For NaEBS, the 3H and 5H shift the most, then 2H and 6H. For the four spectra in the middle, although the peak heights change with the mixing ratio of the two aromatic counterions, their locations barely change. This means that once inserted into the micelles, the two aromatic counterions do not change their penetrating depth or their orientation of penetration, independent of their molar ratio.

Figure 6 shows the surfactant proton chemical shifts for CTAC in the CTAC solutions with the counterion mixtures of NaSal and NaEBS, which are similar in chemical structure. At the very bottom is the CTAC structure with its protons marked. The spectrum above it is the CTAC spectrum without aromatic counterions. The assignment of the CTAC spectrum has been described previously.<sup>11,28</sup> Upon addition of the aromatic counterions, the chemical shifts of the methylene protons *a* through at least *d* are shifted upfield due to the ring current shielding they experience because of the insertion of the aromatic counterions. The *j* protons experience a very small upfield shift, but it is insignificant compared to the *a-d* protons. Chemical shifts of the methylene protons *e* through *h* located further away from the headgroup plus the terminal proton *i*, remain unshifted. All four of the mixed aromatic

counterions spectra show that NaSal and NaEBS penetrate essentially the same distance into the micelles. Changing the ratio between them has no effect on the surfactant's proton chemical shifts.

Figure 7 shows the ring proton chemical shifts for the aromatic counterions of the CTAC with NaSal and NaHN mixture. The spectra on the very top and bottom are for pure NaSal and NaHN in D<sub>2</sub>O without surfactant, respectively. The spectra in between are for a total of 1.5 mM of these two counterions at different ratios with 5 mM CTAC. Upon adding the aromatic counterions to the CTAC solution, all ring protons of both aromatic counterions, except for 1H on NaHN, are shifted upfield, indicating these protons are embedded in the less polar micellar interior. The 1H on NaHN, however, is shifted slightly downfield, suggesting that it lies at or near the water interface and experiences a deshielding effect from the positive headgroups. The orientation of NaHN observed here is consistent with reported data in the literature.<sup>29</sup> Looking at the four mixture spectra from top to bottom, we see that as the ratio of NaSal decreases, its 4, and 3, 5 phenyl protons' chemical shifts move gradually upfield with smaller shifts of 6. In contrast, as the ratio of NaHN decreases, its naphthal protons' chemical shifts move gradually downfield. This suggests that for the mixture of NaSal and NaHN, NaSal penetrates deeper into the surfactant as its concentration decreases while NaHN penetrates less as its concentration increases. These gradual changes are small; however, in comparison to the changes observed when either NaSal or NaHN are initially placed in the environment of the surfactant and we hesitate to overinterpret these observations.

Figure 8 shows the surfactant proton chemical shifts for CTAC in the CTAC solutions with mixtures of NaSal and NaHN. From the spectra we see that NaHN is a deep penetrating counterion because when its concentration is increased, the chemical shifts of CTAC methylene protons *a* up to *g* are shifted upfield more than mixtures with high NaSal to NaHN ratios. The sizes of the shifts are greater for the methylene protons closer to the headgroup. The terminal methyl protons *i* located farthest from the headgroup, which are almost unshifted with NaSal insertion alone, show a small downfield shift after the introduction of NaHN. The precise reason for this downfield shift is not clear, but a referee has suggested that it could be an indication that the surfactant hydrocarbon chain is conformationally flexible and the end of the chain experiences some shielding from the more deeply inserted aromatic group of NaHN and no shielding from the less deeply inserted aromatic group of NaSal.

**ζ Potential and Particle Size.** Table 3 lists the ζ potential and particle size values for the CTAC systems measured by light scattering techniques. The 5 mM CTAC alone in water has a ζ potential of 59 mV and a micellar diameter of 4 nm, which is roughly two times its molecular length indicating it is spherical. Upon addition of aromatic counterions, its ζ potential decreases and its apparent micellar diameter increases dramatically. The synergistic effect of mixed aromatic counterions shows clearly as all mixtures give larger micellar sizes than single counterions (except the 50–50 NaSal and NaHN solution). The ζ potentials of mixed NaSal and NaEBS aromatic counterions do not change much with counterion ratio. However, the ζ potentials decrease markedly with increased NaHN concentration. The 75% and 100% NaHN mixtures give negative ζ potentials. This counterion induced ζ potential charge reversal is very similar to the negative ζ potentials found in CTAC solutions with other strongly binding aromatic counterions, such as sodium 4-iodobenzoate, sodium 4-bromobenzoate, or sodium 4-chlorobenzoate, which are also deeply penetrating counterions.<sup>11</sup> At 100% NaHN, its ζ potential of -21 mV is more negative than that

**Table 3.**  $\zeta$  Potential and Particle Size for CTAC Aqueous Solutions with Mixed Aromatic Counterions

sample (25 °C)	$\zeta$ potential	$\zeta$ potential std. dev.	micelle size
	(mV)	(mV)	(diameter in nm)
CTAC (5 mM)	59	10	4
5 mM CTAC with	100:0	17	70
12.5 mM NaSal: NaEBS	80:20	14	136
60:40	13	3.0	120
40:60	18	3.1	147
20:80	16	3.3	120
0:100	20	5.2	34
5 mM CTAC with	100:0	17	70
12.5 mM NaSal: NaHN	75:25	16	146
50:50	3	4.0	62
25:75	-11	3.1	126
0:100	-21	4.2	55

of CTAT and sodium-4-iodobenzoate, the most electronegative sodium-4-halobenzoate, at the same molar concentrations.

The 50–50 NaSal and NaHN composition has a relatively small micelle size (Table 3) compared to the 75–25 and 25–75 counterion compositions, which is consistent with its moderate drag reduction effectiveness (maximum %DR and maximum  $\tau_{wc}$ ), shown in Table 2.

It should be pointed out that as an indirect-method, light scattering gives particle size results based on model fitting. It can be complicated when the solutions contain more than one type of aggregate. It is likely that spherical surfactant micelles coexist with TLMs of different lengths and different degrees of entanglement or branches or even other large structures such as membranes or liposomes. The particle size distribution for these solutions is typically multimodal with polydispersities around 0.5. This generally suggests that results listed in Table 3 are only comparable to samples measured in the same dispersant and by the same dynamic light scattering techniques. Thus, the particle size measurement values must be treated with caution, but they are useful in indicating trends.

The nanostructural changes induced by the synergistic mixing of aromatic counterions were directly visualized by cryo-TEM of one of the CTAC with mixed aromatic counterion systems as described below.

**Cryo-TEM Images.** Figure 9 shows cryo-TEM images for the 5 mM CTAC aqueous solutions with 12.5 mM mixtures of NaSal and NaEBS at 25 °C. The top two pictures (Figure 9a,b) are for CTAC with the single aromatic counterions NaSal and NaEBS, respectively. TLMs with various lengths are seen in these two pictures. End-caps can be seen in Figure 9b (indicated by black arrows). Some of the TLMs form rings or figure eights (twisted rings). For example, a ring can be seen in Figure 9a (pointed to by a white arrow) and on the left of Figure 9b. A lying 8 can be seen near the bottom of Figure 9b. Slight entanglement can be seen in these two solutions, but there is no apparent branching.

The middle two images (Figure 9c,d) are for 5 mM CTAC aqueous solutions with 12.5 mM mixtures of NaSal and NaEBS at mixing ratios of 20:80 and 80:20, respectively. Branching of TLMs is seen clearly in these two micrographs noted by white arrowheads. For example, one distinct branch is on the upper left of Figure 9c, below which there is a vesicle. The 20:80 solution seems to be more strongly entangled and have more branches than the 80:20 solution. The micellar networks in the ratio 20:80 solution are dominated by Y-junctions with no end-caps seen in the picture while in the ratio

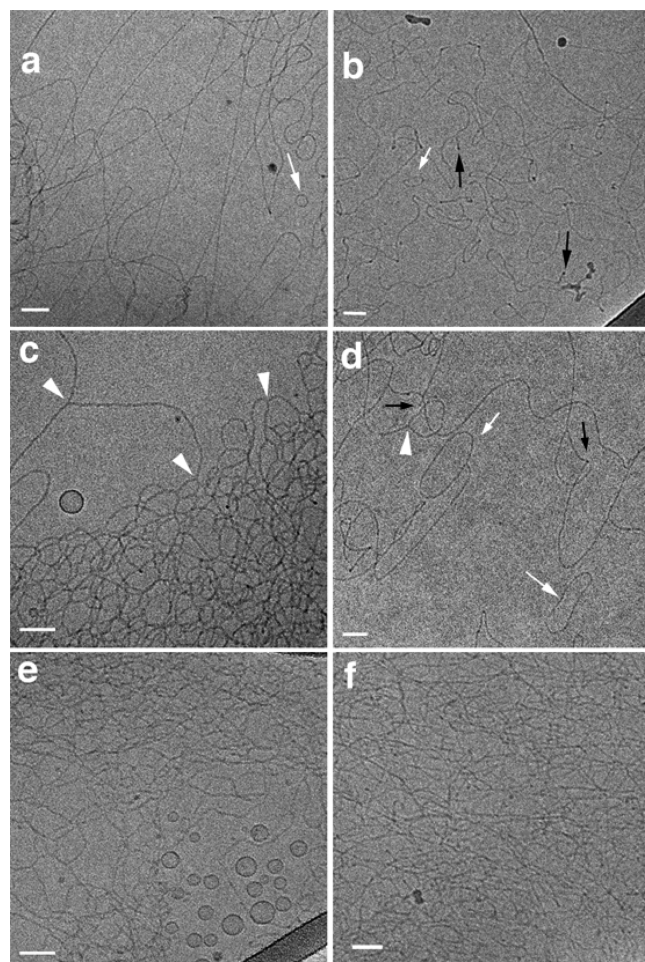


**Figure 9.** Cryo-TEM images of 5 mM CTAC solutions with 12.5 mM mixtures of NaSal and NaEBS. From a–f, the molar ratio of NaSal to NaEBS is as follows: 100 to 0, 0 to 100, 20 to 80, 80 to 20, 40 to 60, and 60 to 40. Arrowheads point to branching points. Black arrows point to TLMs end-caps. White arrows point to closed TLM rings. The dark blotches are specimen surface contamination. All scale bars correspond to 50 nm.

80:20 solution picture, end-caps (pointed to by black arrows), rings (pointed to by white arrows) can be seen.

The bottom two micrographs are for 5 mM CTAC aqueous solutions with mixtures of NaSal and NaEBS at mixing ratios of 40:60 and 60:40, respectively. In the case of these two more evenly mixed aromatic counterion solutions, we observe many branches, forming multiconnected micellar networks, and TLMs which are strongly entangled. The 40:60 solution (Figure 9e) also shows small vesicles.

For these aromatic counterions/CTAC solutions, mixtures of NaSal and NaEBS have more branched and denser micellar networks than pure NaSal and NaEBS. That is, at fixed concentrations of a cationic surfactant and total aromatic counterions, changing the aromatic counterion ratio affects the nanostructure of the TLMs which can be tuned from linear (as shown in images a and b) to branched (as shown in images c and d) and finally to a multiconnected network with many branches (as shown in images e and f).

## ■ ADDITIONAL REMARKS

In addition to the reptation driven by Brownian motions providing a basic way to relieve stress,<sup>30</sup> theoretical, experimental

and molecular simulation investigations have offered a number of stress relief mechanisms unique for surfactant solutions with entangled and/or branched TLM networks: Fast scission and recombination of the entangled TLMs lead to fast relaxation and decreased viscosity.<sup>31–34</sup> Multiconnected or cross-linked networks dominated by branches induce lower viscosity than entangled networks due to the “sliding reptation” or moving junctions, resulting in additional stress relaxation.<sup>35–37</sup> Also, crossing of two entangled TLMs by temporary formation of a four-armed junction at the entanglement point (fusion) followed by junction breakage and the reformation of the original two TLMs, disentangled and stress relieved (“ghost-like crossing model” or “phantom network model”) have been suggested.<sup>15,38–41</sup>

Increased density of branching has been reported to be related to enhancement of the maximum of the elongational viscosity of a surfactant solution in the same manner as in the case of polymer melts,<sup>42</sup> to the fast relaxation of the maximum Trouton ratio for a semidilute mixed surfactant solution,<sup>41</sup> and to higher maximum %DR as well as higher  $\tau_{wc}$  for a cationic surfactant solution.<sup>43</sup> Findings in this work further confirm the positive effect of branching on promoting surfactant micellar network growth and drag reducing effectiveness.

It has long been observed that surfactant solutions may give more drag reduction than polymer solutions.<sup>3,44,45</sup> An example is the maximum drag reduction asymptote (MDRA), which shows the lowest friction factor a solution can achieve with drag reducing additives. The MDRA for surfactants proposed by Zakin et al is about 30% lower than the MDRA for polymers proposed by Virk et al.<sup>3,44,46</sup> This observation may be connected to the fact that branched surfactant micellar solutions have the above-mentioned additional and unique stress relief mechanisms making them more stress resistant and more effective at interacting with microscopic turbulent structures.

## CONCLUSIONS

The conclusions of this work are as follows:

- 1 Cryo-TEM images provided direct visual proof of the effect of the mixed aromatic counterions on branching and multiconnecting of thread-like micelles.
- 2 Due to the additional stress relief mechanisms brought about by the TLM branching, solutions with mixed aromatic counterions showed enhanced drag reduction effectiveness, specifically, expanded EDRTR, increased maximum %DR and enhanced maximum  $\tau_{wc}$ . The increase of the upper temperature limit may be due to enhanced resistance to thermal motions. The decrease of the lower temperature limit may be due to the altered packing in the micelles brought about by the mixed aromatic counterions with different sizes.
- 3 NMR shows that microscopically mixed aromatic counterions both intercalate into micellar interior and exert their counterion function of screening electrostatic charges despite the differences in their binding abilities or sizes. The  $^1\text{H}$  proton on NaHN is shifted downfield, however, suggesting that it lies at or near the water interface.
- 4 Additions of 12.5 mM of pure NaSal or NaEBS counterions (which have similar chemical structures) or their mixtures to 5 mM CTAC decrease  $\zeta$  potential at all counterion mixture molar ratios from 59 mV to the narrow range of 13 to 20 mV. The 80:20, 20:80, 60:40, and 40:60 counterion mixtures significantly increase micelle size compared to either pure counterion, increase branching and multiconnections observed in cryo-TEM images and enhance drag reduction.

5 The strong electronegative NaHN counterion has a very large effect on  $\zeta$  potential even in mixtures with NaSal. When the mixture molar concentration reaches 75% NaHN, the  $\zeta$  potential is negative. At 100% NaHN, its  $\zeta$  potential of -21 mV is more negative than CTAC:Na-p-iodobenzoate at the same molar concentration. The latter is the most electronegative of the Na-p-halobenzoates.<sup>11</sup>

6 The 75:25 and 25:75 mixtures of NaSal:NaHN counterions at 12.5 mM also increase micellar size at 25 °C compared with either counterion alone and enhance drag reduction at 25 °C. The 50:50 mixture, however, has an anomalous small micellar size and associated relatively weak drag reduction behavior at 25 °C.

## AUTHOR INFORMATION

### Corresponding Author

\*Phone: 614-688-4113; Fax: 614-292-3769; E-mail: zakin.1@osu.edu.

## ACKNOWLEDGMENT

W.G. acknowledges the financial support of this work by a Presidential Fellowship and an Alumni Grant for Graduate Research and Scholarship, both from The Ohio State University. Cryo-TEM was performed at Technion-Israel Institute of Technology.

## REFERENCES

- (1) Zakin, J. L.; Lu, B.; Bewersdorff, H.-W. *Rev. Chem. Eng.* **1998**, 14, 253.
- (2) Qi, Y.; Zakin, J. L. *Ind. Eng. Chem. Res.* **2002**, 41, 6326.
- (3) Zakin, J. L.; Zhang, Y.; Ge, W. Drag reduction by surfactant giant micelles. In *Surfactant Science Series*; Zana, R., Kaler Eric, W., Eds., 2007; Vol. 140; pp 473.
- (4) Chou, L. C. Drag-reducing cationic surfactant solutions for district heating and cooling systems. Ph.D Dissertation, The Ohio State University, 1991.
- (5) Rose, G. D.; Foster, K. L. *J. Non-Newtonian Fluid Mech.* **1989**, 31, 59.
- (6) Lin, Z.; Chou, L. C.; Lu, B.; Zheng, Y.; Davis, H. T.; Scriven, L. E.; Talmon, Y.; Zakin, J. L. *Rheol. Acta* **2000**, 39, 354.
- (7) Qi, Y.; Lin, Z.; Mateo, A.; Hart, D. J.; Talmon, Y.; Zakin, J. L. “Investigation of the Odd-Even Effect for Dilute Cationic Surfactant Systems with Salicylate Counterion”; AIChE Annual Meeting, 2000, Los Angeles, CA.
- (8) Qi, Y.; Mateo, A.; Marsteller, W.; Herr, M.; Bass, D.; Hart, D. J.; Talmon, Y.; Zakin, J. L. “Comparison of Cis and Trans Isomer Surfactant-Counterion Systems on Drag Reduction, Rheological Properties and Microstructures”; AIChE Annual Meeting, 2001, Reno, NV.
- (9) Zhang, Y.; Qi, Y.; Zakin, J. L. *Rheol. Acta* **2005**, 45, 42.
- (10) Lin, Z.; Zakin, J. L.; Zheng, Y.; Davis, H. T.; Scriven, L. E.; Talmon, Y. *J. Rheol.* **2001**, 45, 963.
- (11) Ge, W.; Kesselman, E.; Talmon, Y.; Hart, D. J.; Zakin, J. L. *J. Non-Newtonian Fluid Mech.* **2008**, 154, 1.
- (12) Qi, Y. Investigation of relationships among microstructure, rheology, drag reduction and heat transfer of drag reducing surfactant solutions. Ph.D Dissertation, The Ohio State University, 2002.
- (13) Zhang, Y. Correlations among Surfactant Drag Reduction, Additive Chemical Structures, Rheological Properties and Microstructures in Water and Water/Co-solvent Systems. Ph. D. Dissertation, The Ohio State University, 2005.
- (14) Harwigsson, I.; Hellsten, M. *J. Am. Oil Chem. Soc.* **1996**, 73, 921.
- (15) Shikata, T.; Hirata, H.; Kotaka, T. *Langmuir* **1988**, 4, 354.
- (16) Olsson, U.; Soederman, O.; Guering, P. *J. Phys. Chem.* **1986**, 90, 5223.

- (17) Prud'homme, R. K.; Warr, G. G. *Langmuir* **1994**, *10*, 3419.
- (18) Cassidy, M. A.; Warr, G. G. *J. Phys. Chem.* **1996**, *100*, 3237.
- (19) Lindemuth, P. M.; Bertrand, G. L. *J. Phys. Chem.* **1993**, *97*, 7769.
- (20) Rakitin, A. R.; Pack, G. R. *Langmuir* **2005**, *21*, 837.
- (21) Imae, T.; Kohsaka, T. *J. Phys. Chem.* **1992**, *96*, 10030.
- (22) Thalody, B.; Warr, G. G. *J. Colloid Interface Sci.* **1997**, *188*, 305.
- (23) Ge, W.; Zhang, Y.; Zakin, J. L. *Experiments in Fluids* **2007**, *42*, 459.
- (24) Zakin, J. L.; Zhang, Y.; Ge, W. Drag Reduction by Giant Micelles. In *Giant Micelles: Properties and Applications*; Zana, R., Kaler, E. W., Eds.; CRC Press, Taylor and Francis: New York, 2007; Vol. 140; pp 473.
- (25) Talmon, Y. *Surfact. Sci. Ser.* **1999**, *83*, 147.
- (26) Talmon, Y. Seeing giant micelles by cryo-temperature transmission electron microscopy. In *Giant Micelles*; Zana, R., Kaler, E. W., Eds.; CRC Press: New York, 2008.
- (27) Smith, B. C.; Chou, L. C.; Zakin, J. L. *J. Rheol.* **1994**, *38*, 73.
- (28) Rao, U. R. K.; Manohar, C.; Valaulikar, B. S.; Iyer, R. M. *J. Phys. Chem.* **1987**, *91*, 3286.
- (29) Bichofer, S. J.; Simonis, U.; Nowicki, T. A. *J. Phys. Chem.* **1991**, *95*, 480.
- (30) Larson, R. G. *The Structure and Rheology of Complex Fluids*, 1999.
- (31) Kern, F.; Zana, R.; Candau, S. J. *Langmuir* **1991**, *7*, 1344.
- (32) Drye, T. J.; Cates, M. E. *J. Chem. Phys.* **1992**, *96*, 1367.
- (33) Kern, F.; Lequeux, F.; Zana, R.; Candau, S. J. *Langmuir* **1994**, *10*, 1714.
- (34) Rehage, H.; Hoffmann, H. *Mol. Phys.* **1991**, *74*, 933.
- (35) Khatory, A.; Kern, F.; Lequeux, F.; Appell, J.; Porte, G.; Morie, N.; Ott, A.; Urbach, W. *Langmuir* **1993**, *9*, 933.
- (36) Lequeux, F. *Europhys. Lett.* **1992**, *19*, 675.
- (37) Porte, G.; Gomati, R.; El Haitamy, O.; Appell, J.; Marignan, J. *J. Phys. Chem.* **1986**, *90*, 5746.
- (38) Appell, J.; Porte, G.; Khatory, A.; Kern, F.; Candau, S. J. *J. Phys. II* **1992**, *2*, 1045.
- (39) Shikata, T.; Hirata, H.; Kotaka, T. *Langmuir* **1989**, *5*, 398.
- (40) Yamamoto, S.; Hyodo, S.-a. *J. Chem. Phys.* **2005**, *122*, 204907/1.
- (41) Chellamuthu, M.; Rothstein, J. P. *J. Rheol.* **2008**, *52*, 865.
- (42) Fischer, P.; Fuller, G. G.; Lin, Z. *Rheol. Acta* **1997**, *36*, 632.
- (43) Zhang, Y.; Schmidt, J.; Talmon, Y.; Zakin, J. L. *J. Colloid Interface Sci.* **2005**, *286*, 696.
- (44) Zakin, J. L.; Myska, J.; Chara, Z. *AICHE J.* **1996**, *42*, 3544.
- (45) Zakin, J. L.; Ge, W. Polymer and surfactant drag reduction in turbulent flows. In *Polymer Physics: From Suspensions to Nanocomposites to Beyond*; Utracki, L. A., Jamieson, A. M., Eds.; John Wiley & Sons, Inc: New York, 2010; p 776.
- (46) Virk, P. S.; Mickley, H. S.; Smith, K. A. *J. Appl. Mech.* **1970**, *37*, 488.